A comparative analysis of small RNA sequencing data in tubers of purple potato and its red mutant reveals small RNA regulation in anthocyanin biosynthesis

Fang Liu*, Peng Zhao*, Guangxia Chen, Yongqiang Wang and Yuanjun Yang

Institute of Vegetables, Shandong Academy of Agricultural Sciences, Jinan, China

* These authors contributed equally to this work.

ABSTRACT

Anthocyanins are a group of natural pigments acting as stress protectants induced by biotic/abiotic stress in plants. Although the metabolic pathway of anthocyanin has been studied in potato, the roles of miRNAs on the metabolic pathway remain unclear. In this study, a purple tetraploid potato of SD92 and its red mutant of SD140 were selected to explore the regulation mechanism of miRNA in anthocyanin biosynthesis. A comparative analysis of small RNAs between SD92 and SD140 revealed that there were 179 differentially expressed miRNAs, including 65 up- and 114 down-regulated miRNAs. Furthermore, 31 differentially expressed miRNAs were predicted to potentially regulate 305 target genes. KEGG pathway enrichment analysis for these target genes showed that plant hormone signal transduction pathway and plant-pathogen interaction pathway were significantly enriched. The correlation analysis of miRNA sequencing data and transcriptome data showed that there were 140 negative regulatory miRNA-mRNA pairs. The miRNAs included miR171 family, miR172 family, miR530b_4 and novel_mir170. The mRNAs encoded transcription factors, hormone response factors and protein kinases. All these results indicated that miRNAs might regulate anthocyanin biosynthesis through transcription factors, hormone response factors and protein kinase.

Subjects Agricultural Science, Molecular Biology, Plant Science

Keywords Purple potato, Red mutant, Small RNA, Anthocyanin

INTRODUCTION

Anthocyanins are flavonoid compounds, which are secondary metabolites. They are natural food pigments found in edible parts of fruits, vegetables and crops (*Chiu et al., 2010*). The foods rich in anthocyanin present bright colors and are popular with people (*Bimpilas et al., 2016*). Moreover, anthocyanins also have antioxidant activity and can protect human beings from disease or reduce the damage of disease. The anthocyanin extracts from purple rice protect cardiac function in STZ-induced diabetes rat hearts by inhibiting cardiac hypertrophy and fibrosis (*Chen et al., 2016*). Anthocyanins from red potato show anti-hepatotoxity in rats with toxicity of D-galactosamine (*Han et al., 2006*).

Submitted 15 April 2022
Accepted 13 April 2023
Published 19 May 2023

Corresponding author
Yuanjun Yang, yangyuanjun@263.net.cn

Academic editor
Rana Muhammad Atif

Additional Information and Declarations can be found on page 15

DOI **10.7717/peerj.15349**

How to cite this article Liu F, Zhao P, Chen G, Wang Y, Yang Y. 2023. A comparative analysis of small RNA sequencing data in tubers of purple potato and its red mutant reveals small RNA regulation in anthocyanin biosynthesis. *PeerJ* **11**:e15349
http://doi.org/10.7717/peerj.15349

Anthocyanin extracts from bilberries and blackcurrants have protective activity on acute acetaminophen-induced hepatotoxicity in rats (*Cristani et al., 2016*).

In anthocyanin biosynthesis, phenylalanine is a primary precursor. Then under the action of a series of enzymes, the substances of coumaroyl CoA, dihydroflavonols, leucoanthocyanins and anthocyanins are successively produced. Anthocyanin biosynthesis is regulated by structural genes and their transcription factors. Some genes regulating anthocyanin biosynthesis have been isolated and characterized in potato, such as *f3'5'h* (*Jung et al., 2005*), *dfr* (*De Jong et al., 2003*), *developer* (*D*) locus (*Jung et al., 2009*), *AN1* (*D'Amelia et al., 2014*) and *StMYB44* (*Liu et al., 2019*).

Small RNAs usually consist of 20-30 nucleotides and widely exist in eukaryotic organisms. According to their biogenesis modes, small RNAs are distinguished into three major types, namely miRNA, siRNA and piRNA (*Axtell, 2013*; *Chen, 2009*). Small RNAs guide biological processes at DNA or RNA level, for example, the cleavage of complementary RNAs. Different types of small RNAs have similar molecular functions. Both miRNAs and siRNAs can inhibit translation of target mRNAs, and both siRNAs and piRNAs can direct chromatin modifications (*Chen, 2009*). miRNAs regulate target mRNAs through transcript cleavage and/or translational inhibition. Conserved miRNAs play vital roles in many plant physiological processes, such as development, stress responses, primary and secondary metabolism (*Gou et al., 2011*; *Jones-Rhoades, Bartel & Bartel, 2006*; *Matzke et al., 2009*; *Xia et al., 2012*).

So far, miRNAs have been proved to be involved in the regulation of anthocyanin biosynthesis. miRNA858a and HYPOCOTYL 5 (HY5) can repress the expression of *MYB-LIKE 2* (*MYBL2*), thus leading to the activation of anthocyanin biosynthesis pathway (*Wang et al., 2016*). Increasing miR156 activity promotes anthocyanin accumulation, while reducing miR156 activity leads to a high level of flavonol (*Gou et al., 2011*). Both miR828 and miR858 regulate *VvMYB114* to promote anthocyanin biosynthesis in grapes (*Tirumalai et al., 2019*). The miRNA involved in anthocyanin biosynthesis pathway are also reported in apple (*Hu et al., 2021*), tomato (*Jia et al., 2015*), potato (*Bonar et al., 2018*) and kiwifruit (*Li et al., 2019*). However, there are few studies on the post-transcriptional regulation of miRNA in potato anthocyanin biosynthesis. In the study, a comparative miRNA analysis and the expression analysis of miRNA-mRNA were performed between purple flesh potato, SD92, and its red flesh mutant, SD140. These results will shed light on the regulation mechanism of miRNA in potato anthocyanin biosynthesis.

MATERIALS & METHODS

Plant materials

SD92, commonly known as Hei Jingang, was a tetraploid potato with purple skin and purple flesh. SD140 is a mutant of SD92. Its skin and flesh colors were red (*Liu et al., 2018*; *Liu et al., 2015*). Two materials were planted in a greenhouse for two months at 20 $\pm$ 2 °C with a photoperiod of 16 h light/8 h dark.

Sample library construction and sequencing

Fresh tubers (diameter 4–5 cm) from three individual plants were harvested for three biological replicates, cleaned with sterilized water, frozen in liquid nitrogen and finally stored at −80 °C. Total RNA extraction of the samples was performed with a modified Trizol reagent (*Liu et al., 2018*) for library construction and validation of miRNA sequencing data.

Small RNA was isolated and the library was constructed in accordance with the protocol of Preparing Samples for Analysis of Small RNA (Illumina, San Diego, CA, USA). The 18-30 nt RNA segments were separated from total RNA by polyacrylamide gel electrophoresis, then ligated with 3′ adaptor (GAACGACATGGCTACGATCCGACTT) and 5′ adaptor (AGTCGGAGGCCAAGCGGTCTTAGGAAGACAA). The resulting segments were employed to synthesize first-strand cDNA. The cDNA was amplified and only cDNA with both 3′ and 5′ adaptors was enriched. Finally, the fragments of 100–120 bp were separated to construct the library. After library quantification and single-stranded DNA cyclization, the library was sequenced by BGISEQ-500 technology. The raw data was deposited into NCBI BioProject database (PRJNA824931).

miRNA identification and prediction

The impurities of raw data, including 5′ primer contaminants, no-insert tags, oversized insertion tags, low quality tags, poly-A tags and the tags without 3′ primer, were excluded from the raw data to obtain clean tags. Low-quality tags were tags whose base quality values were less than 20, accounting for more than 50% of the total bases. The clean tags were mapped to potato reference genome PGSC_DM v4.03 (http://solanaceae.plantbiology.msu.edu/data) by Bowtie2 (*Langmead et al., 2009*) and small RNA databases miRBase (*Kozomara & Griffiths-Jones, 2014*), snoRNA (*Yoshihama, Nakao & Kenmochi, 2013*) and Rfam (*Nawrocki et al., 2015*). If a small RNA could be mapped to more than one database, the small RNA annotation followed the searching priority of miRBase > snoRNA > Rfam. One small RNA was only mapped to one category. The small RNAs mapped to Rfam database were validated by cmsearch (*Nawrocki & Eddy, 2013*). The novel miRNA was determined by miRA (*Evers et al., 2015*) according to the characteristic hairpin structure of miRNA precursor. Small interfering RNA (siRNA), a 22–24 nt double-strand RNA, was identified by the characteristic of one strand 2 nt shorter than the other (*Jagla et al., 2005*).

miRNA expression and screening of differentially expressed miRNAs (DEMs)

The expression level of miRNA was estimated by the transcripts per kilobase million (TPM) (*'t Hoen et al., 2008*). The differential expression was calculated by DEGseq (*Wang et al., 2010*) based on MA-plot method (*Yang et al., 2002*). The *P*-value calculated for each gene was adjusted to Q-value for multiple testing corrections by two alternative strategies. The miRNAs with expression fold change > 2 and Q-value < 0.001 were defined as differentially expressed miRNAs. The volcano plot and heatmap of differentially expressed miRNAs were obtained by Excel 2016 and MeV (*Saeed et al., 2003*), respectively.

Table 1 Primer sequences of miRNAs for real-time quantitative PCR.

Primer	Direction	Sequence (5′–3′)
18S rRNA	Forward	CCTGGTCGGCATCGTTTA
18S rRNA	Reverse	CGAACAACTGCGAAAGCAT
miR156a-5p	Forward	TGACAGAAGAGAGTGAGCAC
miR166a-3p	Forward	TCGGACCAGGCTTCATTCC
miR166d-5p_2	Forward	GGAATGTTGTCTGGCTCGAGG
miR171b-3p	Forward	TTGAGCCGTGCCAATATCAC
miR171b-3p_2	Forward	TTGAGCCGCGTCAATATCTCT
miR172b	Forward	GGAATCTTGATGATGCTGCA
miR172e-5p	Forward	GCAACATCATCAAGATTCACA
miR399a_6	Forward	GCCAAAGGAGAATTGCCCTG
miR399i	Forward	CCAAAGGAGAGCTGCCCTG
miR399j_2	Forward	TGCCAAAGGAGAGTTGCCCTA
miR530a	Forward	TGCATTTGCACCTGCACCTT
miR828a_1	Forward	CGCTGTCTTGCTCAAATGAGTATTC
novel_mir32	Forward	ATTAACTTTGGCCAGCATC
novel_mir105	Forward	GGACCCTTGGCGAAGTCACC
novel_mir143	Forward	CACTGAGTTGGACCCTTGGC
novel_mir170	Forward	GCGAGCGAATTAGATTCATTGTTTGA

Target gene prediction, Gene Ontology (GO) and KEGG pathway enrichment analyses

TargetFinder (*Fahlgren & Carrington, 2010*) and psRobot (*Wu et al., 2012*) were used to predict the target genes of miRNAs. All target genes were mapped to GO-terms in the database (http://www.geneontology.org/) and KEGG Orthology (*Kanehisa et al., 2008*) pathways. The enrichment analyses of GO terms and KEGG pathways were performed by the hypergeometric test based on GO::TermFinder (*Boyle et al., 2004*). The *P*-values were adjusted by Bonferroni method (*Abdi, 2007*). The adjusted *P*-value was defined as Q-value. The terms with Q-value < 0.05 were defined as significantly enriched terms.

Expression validation of miRNAs

RNAs were digested by DNaseI (Thermo, USA) to remove genome DNA. First-strand cDNA was synthesized by miRNA First Strand cDNA Synthesis Kit (Sangon Biotech, China) using tailing reaction method. Real-time quantitative PCR (RT-qPCR) was performed with UltraSYBR Mixture Kit (CWBIO, China) by using *18S rRNA* (GenBank: X67238.1) as a reference gene. The primers of *18S rRNA* and miRNAs were listed in Table 1. The universal reverse primer for miRNAs was supplied from miRNA First Strand cDNA Synthesis Kit. Three biological replicates were performed. Significant difference of miRNA expression between SD92 and SD140 was identified by Student's *t*-test ($P < 0.05$).

Table 2 Summary of sequencing data for each sample.

Sample name	Raw tag count	Low quality tag	Invalid adapter tag	Poly A tag	Tag length < 18	Clean tag	Q20 of clean tag (%)	Percentage of clean tag (%)
SD140_1	30,152,601	521,573	1,211,217	765	296,890	28,122,156	99.30	93.27
SD140_2	29,662,224	559,145	642,637	1,307	285,077	28,174,058	99.20	94.98
SD140_3	29,108,569	439,201	1,438,318	979	420,200	26,809,871	99.20	92.10
SD92_1	28,058,311	476,281	601,154	814	262,128	26,717,934	99.00	95.22
SD92_2	28,907,701	462,036	684,333	2,174	265,810	27,493,348	99.30	95.11
SD92_3	29,706,600	544,647	816,486	1,600	341,405	28,002,462	99.20	94.26

RESULTS

Sequencing and classification of potato small RNAs

To identify the miRNAs regulating potato flesh color, six small RNA libraries were constructed and sequenced. The counts of raw tags of six libraries ranged from 28,058,311 to 30,152,601 (Table 2). Low quality tags, invalid adapter tags, poly-A tags and short valid length tags (shorter than 18 nt) were removed to obtain clean tags. The percentages of clean tags of six libraries ranged from 92.10% to 95.22%, which indicated the sequencing data could be used for subsequent analyses. Of the six libraries, 19-25 nt length tags accounted for 87.9%–96.4% of the total tags, and the 24 nt tags were the most abundant (Table S1). More than 85.04% of the total clean tags from six libraries were mapped to the reference genome (Table S2). Therefore, the sequencing data should accurately reflect small RNA expression and could be used for differential expression analysis of small RNA. To classify and annotate small RNAs, the clean tags were mapped to small RNA databases miRBase, snoRNA and Rfam. The types and proportion of identified small RNAs were similar within six libraries. The intergenic miRNAs were the most abundant (Table S3).

Identification of known and novel miRNAs

There were about 300 known miRNAs and 160 novel miRNAs identified in every library (Table 3). In total, 356 known miRNAs belonging to 121 miRNA families were identified (Table S4), and miR172 family was the most abundant family where 21 members were identified. The nucleotide bias analyses on these non-redundant known miRNAs (Fig. S1A) showed that the first and 24th nucleotide preferred to be uracil (U), and adenine (A) was the dominant nucleotide in the 10th nucleotide position. Meanwhile, several nucleotide positions were conserved. For example, the proportions of four kinds of nucleotides were nearly equal in the 4th, 9th and 16th nucleotide position (Fig. S1A).

Unmapped tags were further used to predict novel small RNAs. Totally, 171 novel miRNAs were identified for six libraries. The mature sequences, star sequences and precursor sequences of 171 novel miRNAs were listed in Table S5. The length of the novel miRNAs ranged from 19 to 30 nucleotides. Most of the nucleotide positions preferred to be uracil (U) or adenine (A) (Fig. S1B). Two exceptions were the 9th and 11th nucleotide where the dominant nucleotides were guanine (G) and cytosine (C), respectively.

Table 3 Summary of detected small RNAs for each sample.

Sample name	Known miRNA	Novel miRNA	Known siRNA	Novel siRNA
SD140_1	290	151	0	12,518
SD140_2	293	161	0	13,671
SD140_3	284	145	0	12,447
SD92_1	275	166	0	13,373
SD92_2	304	161	0	11,225
SD92_3	311	168	0	13,147

Differentially expressed miRNAs between SD92 and SD140

To further validate the expression changes of miRNAs between SD92 and SD140, 15 miRNAs from 11 different miRNA families were randomly selected to be tested by RT-qPCR (Fig. 1). The results of RT-qPCR showed the same expression regulation pattern with miRNA sequencing data, which suggested that the miRNA sequencing result was reliable. What's more, the results showed 6 miRNAs were differentially expressed between SD92 and SD140 ($P < 0.05$). Different miRNAs from the same miRNA family displayed the same regulation pattern. For example, both miR166a-3p and miR166d-5p_2 were from miR166 family and exhibited higher expression levels in SD140 than in SD92.

A total of 179 differentially expressed miRNAs were identified in this study, including 107 known miRNAs and 72 novel miRNAs (Fig. 2A, Table S6). Among the differentially expressed miRNAs, 65 and 114 were confirmed to be up- and down-regulated in SD140, respectively. These miRNAs belonged to 49 miRNA families. Of the 49 miRNA families, miR399 and miR172 family were the two largest families, which contained 10 and 9 miRNA members, respectively. Interestingly, the members of miR399 and miR172 families were significantly down-regulated in SD140, respectively.

Target gene prediction of miRNAs

To further explore the function of miRNAs, the target genes (mRNAs) of all miRNAs were predicted by psRobot and TargetFinder. Totally, 7,416 target genes were identified for 450 miRNAs where 897 target genes were confirmed as targets of 116 miRNAs by both softwares. Among these 897 target genes, 305 genes were regulated by 31 differentially expressed miRNAs (Table S7).

GO and KEGG pathway enrichment analysis of target genes

GO enrichment analysis of the above 305 target genes showed that the biological process ontology included 47 GO terms. "Cellular macromolecule metabolic process" and "macromolecule metabolic process" were the most abundant GO terms, containing 77 genes, respectively.

The cellular component ontology included 16 GO terms, and the most abundant terms were "cell" and "cell part", which contained 115 genes, respectively. The molecular

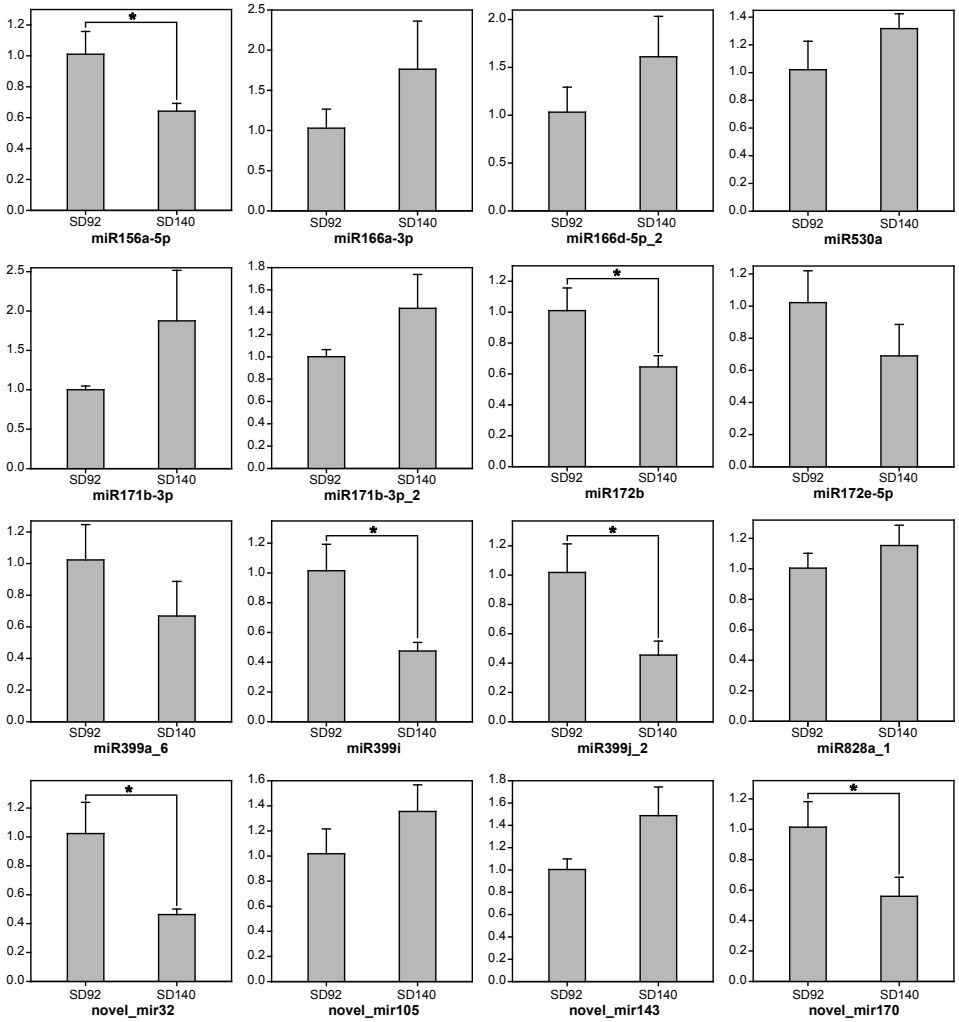

Figure 1 Expression analysis of miRNAs by RT-qPCR. The values are represented by mean ± standard deviation ($n = 3$). Student's t-test, $P < 0.05$.

Full-size DOI: 10.7717/peerj.15349/fig-1

function ontology included 10 GO terms. The GO term "binding" contained 126 genes, which was the most abundant term in molecular function (Fig. 3).

To explore the possible function of target genes, KEGG pathway enrichment analysis was performed. The 305 target genes of 31 DEMs were distributed in 6 first-level and 33 second-level KEGG pathways, respectively. The first-level KEGG pathway term "metabolism" was the most abundant, including 10 second-level KEGG pathway terms. Thirty-eight target genes were assigned in the second-level KEGG pathway term "signal transduction", which was the most abundant second-level KEGG pathway term (Fig. 4).

Among the enriched top 20 pathways, only two pathways, "plant hormone signal transduction" and "plant-pathogen interaction", were defined as significantly enriched pathways ($P < 0.05$), which comprised 24 target genes, respectively (Fig. 5 and Table

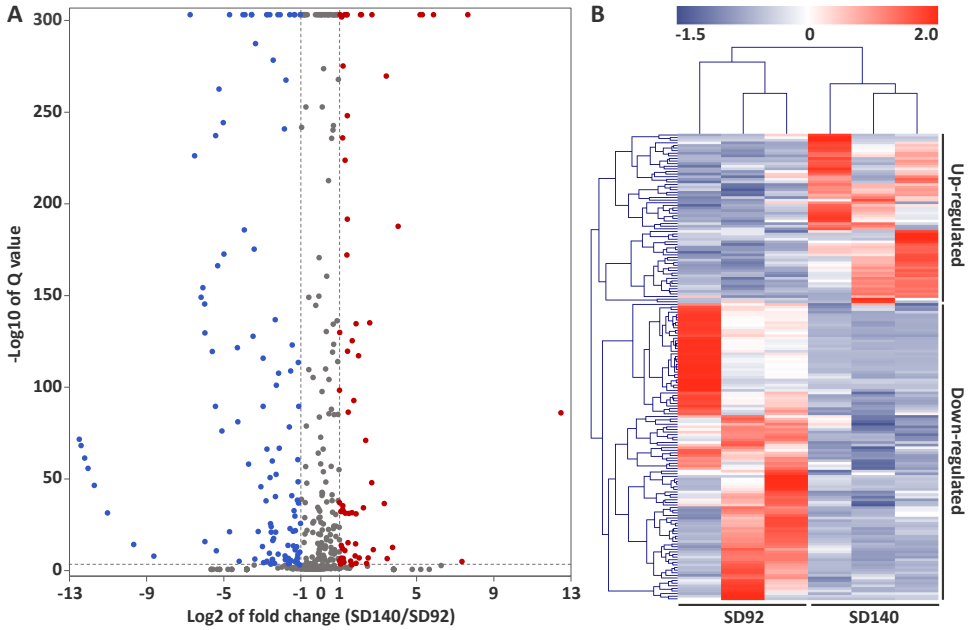

Figure 2 Identification of differentially expressed miRNAs between SD92 and SD140. (A) Volcano plot of differentially expressed miRNAs between SD92 and SD140. The cutoff values of fold change and *Q*-value are > 2 and < 0.001, respectively. Up-regulated and down-regulated miRNAs are indicated by red and blue dots. (B) Heatmap of differentially expressed miRNAs in three biological replicates. Hierarchical clustering was performed by complete linkage method and Euclidean distance.

Full-size DOI: 10.7717/peerj.15349/fig-2

S8). This indicated that the DEMs between SD92 and SD140 might be involved in plant-pathogen interaction and hormone signal transduction.

Target genes of miRNAs involved in regulation of anthocyanin biosynthesis

Generally, plant miRNAs regulate target mRNAs through two major mechanisms, transcript cleavage and translational inhibition (*Chen, 2009*), thus there are negative regulation relationship in the expressions of miRNA and corresponding target genes. In our previous study, a comparative transcriptome analysis was performed between SD92 and SD140 (*Liu et al., 2018*). By combining transcriptome sequencing data (SRA accession number: SRP125987) and miRNA sequencing data of present study, 31 differentially expressed miRNAs and corresponding target mRNAs were identified and listed in Table S9. Among them, the differentially expressed miRNAs negatively regulating target mRNAs were screened, and 140 miRNA-mRNA pairs were confirmed. In these miRNAs-mRNAs pairs, miRNAs contained 5 known miRNA families and 12 novel miRNAs. These mRNAs corresponded to 71 genes (Table 4). These genes mainly encoded transcription factors, quamosa promoter binding protein, hormone response factors, protein kinases and disease resistance protein.

Transcription factors affect anthocyanin biosynthesis by regulating the expressions of structural genes (*D'Amelia et al., 2014*; *Liu et al., 2016*). In this study, we focused on the regulation of miRNA on transcription factors in anthocyanin biosynthesis (Table 4).

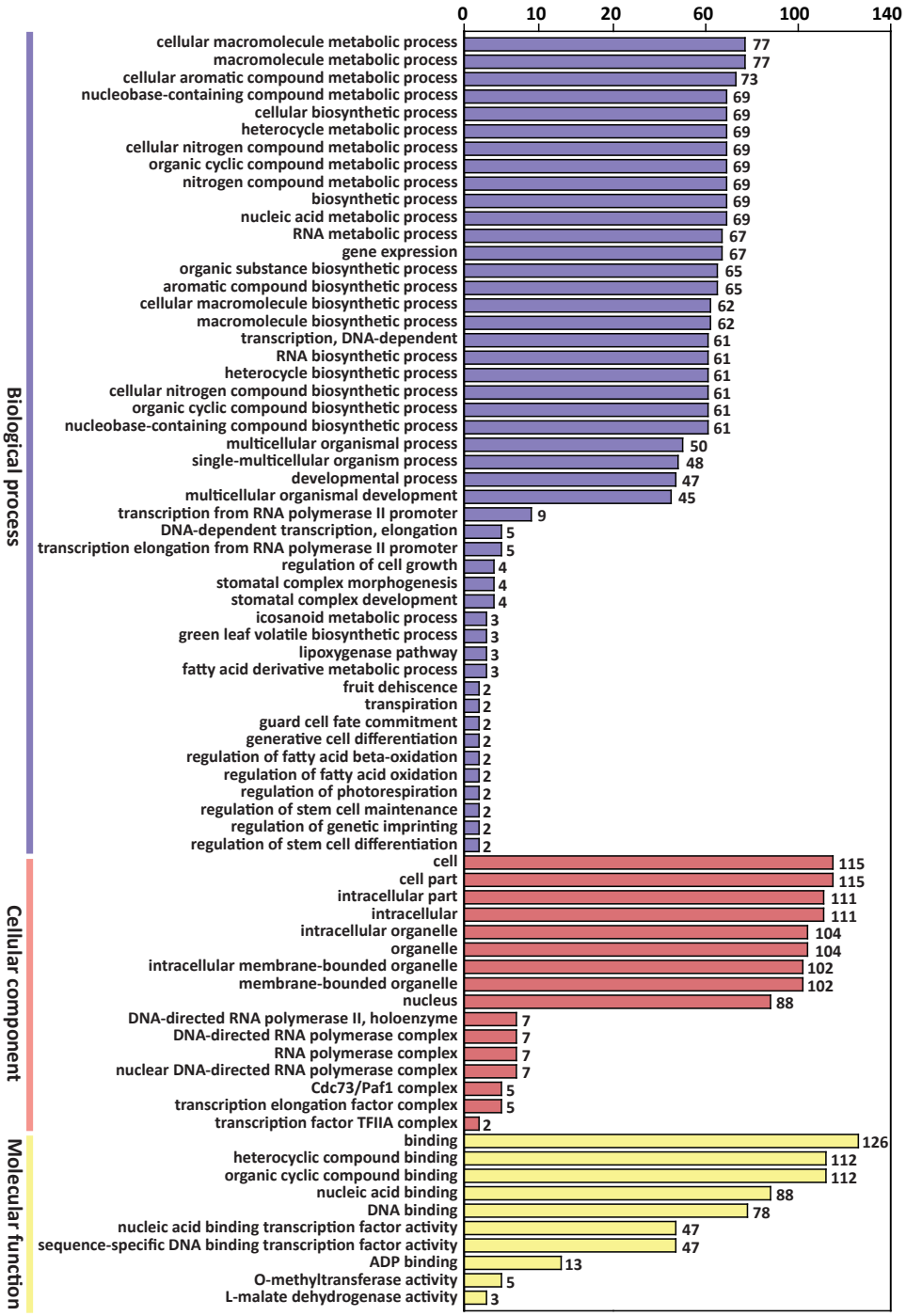

Figure 3 **GO classification of predicted target genes of the differentially expressed miRNAs.**
Full-size DOI: 10.7717/peerj.15349/fig-3

PGSC0003DMG400006604, *PGSC0003DMG400011046* and *PGSC0003DMG400012038*, which were regulated by miR172b, encoded AP2 transcription factor SlAP2e, RAP2-7-like and RAP2-7, respectively. The target gene of miR530b_4, *PGSC0003DMG400025479*,

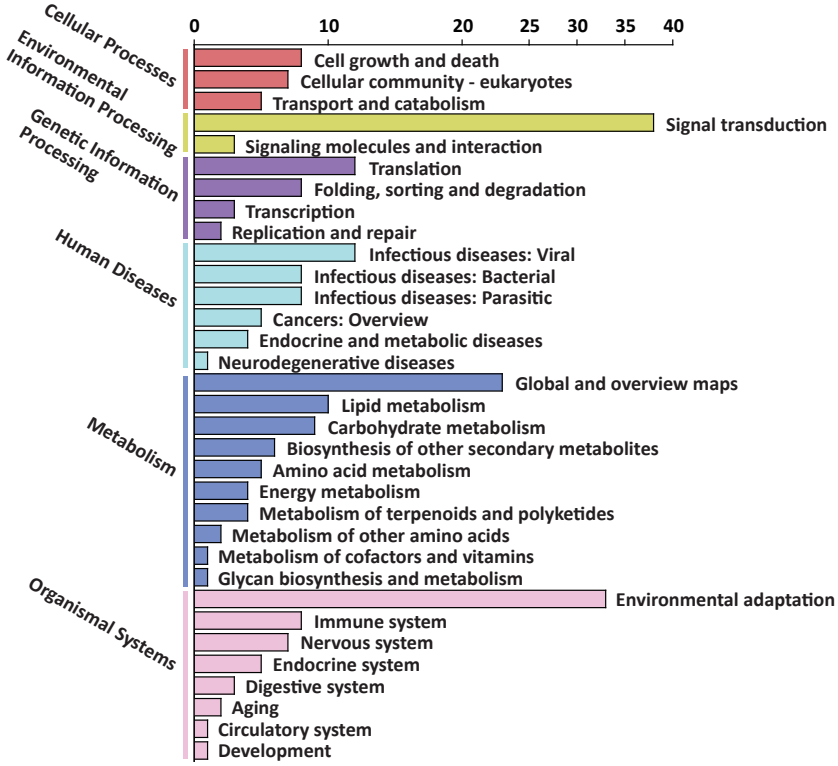

Figure 4 First-level and second-level KEGG pathway classification of predicted target genes of the DEMs. Six different first-level KEGG pathway are distinguished in different colors.

Full-size DOI: 10.7717/peerj.15349/fig-4

encoded AP2-like transcription factor TOE3. *PGSC0003DMG400011457* encoded WRKY transcription factor 48 and was regulated by miR172e-5p. Both *PGSC0003DMG400004826* and *PGSC0003DMG400018279*, which were regulated by novel_mir170, encoded transcription factor ERF039-like and MYB35-like, respectively.

Hormones improve the biosynthesis of anthocyanins (*Zhang et al., 2011*; *Palma-Silva et al., 2016*), so we did research on miRNA regulating hormones in this experiment in order to throw light on miRNA regulation mechanism on anthocyanins biosynthesis. In this study, RAP2-7 and RAP2-7-like, which were regulated by miR172b, were ethylene-responsive transcription factors. TOE3 transcription factor, which was regulated by miR172b and miR530b_4, was also responsive to ethylene (Table 4). The target gene of miR171b-3p, *PGSC0003DMG400012683*, encoded the DELLA protein that was an inhibitor of GA signal transduction.

Protein kinases are involved in anthocyanin biosynthesis (*Li et al., 2016*). Protein kinases regulated by miRNA were investigated in this study. Both *PGSC0003DMG400018811* and *PGSC0003DMG400024795*, which were regulated by novel_mir170, encoded LRR receptor-like serine/threonine protein kinase ERECTA and RCH1, respectively. *PGSC0003DMG400026383* encoded receptor-like protein kinase and was regulated by novel_mir117.

Figure 5 **Scatterplot of enriched KEGG pathways of predicted target genes of the DEMs.** *X* axis indicates the rich factor. The rich factor is the ratio of DEMs target gene numbers annotated in the pathway term to all gene numbers annotated in the pathway. *Y* axis indicates KEGG pathways.
Full-size DOI: 10.7717/peerj.15349/fig-5

There were also significant changes in the expression of target genes regulated by other miRNAs, such as *PGSC0003DMG402007414*, which was target gene of novel_mir105 and novel_mir143, but the gene function was unknown.

DISCUSSION

Generally, miRNAs play an important role in some kinds of plant biological processes such as growth, development and stress response (*Jones-Rhoades, Bartel & Bartel, 2006*). The functions of miRNAs in plant anthocyanin biosynthesis have been reported in some species, including Arabidopsis (*Gou et al., 2011*; *Wang et al., 2016*), apple (*Hu et al., 2021*), grape (*Tirumalai et al., 2019*), tomato (*Jia et al., 2015*), sweet potato (*He et al., 2019*) and kiwi fruit (*Li et al., 2019*).

Table 4 Differentially expressed miRNAs and negatively regulated target genes.

miRNA	Target gene	Gene annotation
miR156a-5p	*PGSC0003DMG400022824*	Squamosa promoter-binding protein 1-like
miR156a-5p	*PGSC0003DMG400023962*	Uncharacterized protein
miR156a-5p	*PGSC0003DMG400029156*	Cell cycle checkpoint protein RAD17
miR156a-5p	*PGSC0003DMG400032817*	Squamosa promoter-binding protein 1-like
miR156a-5p	*PGSC0003DMG400034310*	Squamosa promoter-binding-like protein 12
miR171b-3p	*PGSC0003DMG400009015*	DEAD-box ATP-dependent RNA helicase 24
miR171b-3p	*PGSC0003DMG400012683*	DELLA protein
miR172b	*PGSC0003DMG400004006*	Floral homeotic protein APETALA 2
miR172b	*PGSC0003DMG400006604*	AP2 transcription factor SlAP2e
miR172b	*PGSC0003DMG400011046*	Ethylene-responsive transcription factor RAP2-7-like
miR172b	*PGSC0003DMG400012038*	Ethylene-responsive transcription factor RAP2-7
miR172b	*PGSC0003DMG400027904*	Floral homeotic protein APETALA 2-like
miR172b	*PGSC0003DMG400030080*	Phosphatidylinositol/phosphatidylcholine transfer protein SFH4
miR172b & miR530b_4	*PGSC0003DMG400025479*	AP2-like ethylene-responsive transcription factor TOE3
miR172e-5p	*PGSC0003DMG400010386*	Malate dehydrogenase, glyoxysomal
miR172e-5p	*PGSC0003DMG400011457*	Probable WRKY transcription factor 48
miR172e-5p	*PGSC0003DMG400011477*	Putative lysine-specific demethylase JMJ16
miR172e-5p	*PGSC0003DMG400021020*	Uncharacterized protein
miR172e-5p & novel_mir32	*PGSC0003DMG400014214*	Uncharacterized protein
miR482e-5p & novel_mir117	*PGSC0003DMG400030780*	Uncharacterized protein
miR530a	*PGSC0003DMG400010027*	Dof zinc finger protein DOF3.5-like
miR530a	*PGSC0003DMG400022193*	Pirin-like protein
miR530a	*PGSC0003DMG400030421*	Transcription initiation factor IIA large subunit
miR530a	*PGSC0003DMG400038860*	Uncharacterized protein
miR530b_4	*PGSC0003DMG400001126*	Uncharacterized protein
miR530b_4	*PGSC0003DMG400030587*	Non-specific lipid-transfer protein 2-like
novel_mir32	*PGSC0003DMG400003436*	Uncharacterized protein
novel_mir32	*PGSC0003DMG400007187*	Probable protein S-acyltransferase 1
novel_mir32	*PGSC0003DMG400009055*	Uncharacterized protein
novel_mir32	*PGSC0003DMG400011113*	Putative disease resistance protein RGA3
novel_mir32	*PGSC0003DMG400012875*	Protein disulfide isomerase-like 1-3
novel_mir32	*PGSC0003DMG400016798*	Polyadenylate-binding protein 2-like
novel_mir32	*PGSC0003DMG400017569*	Protein disulfide-isomerase-like
novel_mir32	*PGSC0003DMG400027301*	Caffeic acid 3-O-methyltransferase-like
novel_mir32	*PGSC0003DMG400032155*	Linoleate 13S-lipoxygenase 2-1, chloroplastic
novel_mir32	*PGSC0003DMG400043688*	Uncharacterized protein
novel_mir42	*PGSC0003DMG400008897*	L-type lectin-domain containing receptor kinase IV.1-like
novel_mir54	*PGSC0003DMG400032120*	UPF0496 protein At3g19330-like
novel_mir61	*PGSC0003DMG400004296*	Late blight resistance protein homolog R1B-16

(*continued on next page*)

Table 4 (*continued*)

miRNA	Target gene	Gene annotation
novel_mir61	*PGSC0003DMG400004756*	Late blight resistance protein homolog R1A-10
novel_mir61	*PGSC0003DMG400007867*	Disease resistance protein RGH3
novel_mir61	*PGSC0003DMG400007870*	Late blight resistance protein homolog R1A-3
novel_mir61	*PGSC0003DMG400007872*	Late blight resistance protein homolog R1C-3
novel_mir61	*PGSC0003DMG400031244*	THUMP domain-containing protein 1 homolog
novel_mir61	*PGSC0003DMG402007871*	Disease resistance protein RGH3
novel_mir67	*PGSC0003DMG400008560*	Uncharacterized protein
novel_mir67	*PGSC0003DMG400017053*	Uncharacterized protein
novel_mir67	*PGSC0003DMG400030551*	Multicopper oxidase LPR2
novel_mir75	*PGSC0003DMG400003887*	Uncharacterized protein
novel_mir75	*PGSC0003DMG400009731*	Probable S-adenosylmethionine-dependent methyltransferase
novel_mir75	*PGSC0003DMG400017312*	RING finger protein 44
novel_mir75	*PGSC0003DMG400025978*	Uncharacterized protein
novel_mir78	*PGSC0003DMG400000774*	RNA-binding protein 2
novel_mir89	*PGSC0003DMG400006945*	Senescence-associated carboxylesterase 101-like
novel_mir105 & novel_mir143	*PGSC0003DMG402007414*	Uncharacterized protein
novel_mir117	*PGSC0003DMG400020645*	ycf54-like protein
novel_mir117	*PGSC0003DMG400026383*	Probable receptor-like protein kinase
novel_mir117	*PGSC0003DMG400031180*	Uncharacterized protein
novel_mir128	*PGSC0003DMG400034633*	Uncharacterized protein
novel_mir128	*PGSC0003DMG400037457*	Uncharacterized protein
novel_mir128	*PGSC0003DMG400043850*	Uncharacterized protein
novel_mir170	*PGSC0003DMG400000513*	Galactinol-sucrose galactosyltransferase 5
novel_mir170	*PGSC0003DMG400002541*	60S ribosomal protein L37-3
novel_mir170	*PGSC0003DMG400004826*	Ethylene-responsive transcription factor ERF039-like
novel_mir170	*PGSC0003DMG400007189*	Proteasome subunit alpha type-3-like, partial
novel_mir170	*PGSC0003DMG400008432*	Uncharacterized protein
novel_mir170	*PGSC0003DMG400012159*	KAT8 regulatory NSL complex subunit 3
novel_mir170	*PGSC0003DMG400018279*	Transcription factor MYB35-like
novel_mir170	*PGSC0003DMG400018811*	LRR receptor-like serine/threonine-protein kinase ERECTA
novel_mir170	*PGSC0003DMG400024795*	LRR receptor-like serine/threonine-protein kinase RCH1
novel_mir170	*PGSC0003DMG400033933*	Hypothetical protein SDM1_41t00024

In this study, miR399 and miR172 families were the two largest differentially expressed miRNA families. The expressions of miR399 family (miR399a_6, miR399i, miR399j_2) and miR172 family (miR172e-5p, miR172b) were down-regulated in SD140. miR172 inhibits flavonoid biosynthesis through suppressing the expression of an AP2 transcription factor that positively regulates *MdMYB10* (*Ding et al., 2022*). In SD140, miR172b was down-regulated, and its target gene encoding AP2-like factor was up-regulated, indicating that miR172b regulated the change in anthocyanin biosynthesis from petunidin to pelargonidin through AP2-like factor. Both miR399 expression and anthocyanin accumulation are increased under Pi-deficiency conditions (*Chen et al., 2018*; *Hsieh et al., 2009*). miR399 is related to anthocyanin accumulation. However, the target gene of miR399 was unknown

in SD92 and SD140, so the regulation mechanism of miR399 in anthocyanin biosynthesis remains unclear and needs further study.

miR171 family (miR171a-3p, miR171b-3p, miR171b-3p_2) was up-regulated in SD140 (Table S6). miR171 is down-regulated and anthocyanin accumulation is up-regulated under water deficit (*Ghorecha et al., 2014*). miR171 is related with anthocyanin accumulation. The target gene of miR171b-3p, *PGSC0003DMG400012683*, encoded DELLA protein. DELLA proteins are important repressors of GA signaling (*Chai et al., 2022*; *Sukiran et al., 2022*). Plant hormones are involved in anthocyanin biosynthesis, such as auxin (*Ji et al., 2015*; *Liu, Shi & Xie, 2014*), abscisic acid (ABA) (*Balint & Reynolds, 2013*; *Leão et al., 2014*) and gibberellic acid (GA) (*Loreti et al., 2008*). GA represses the sucrose accumulation in anthocyanin synthesis (*Loreti et al., 2008*) and decreases anthocyanin accumulation under low temperature or phosphate starvation (*Jiang et al., 2007*; *Zhang et al., 2011*). Moreover, the KEGG pathway ''plant hormone signal transduction'' comprising of 24 target genes was significantly enriched in this study, which suggested that plant hormones were involved in the anthocyanin biosynthesis in SD92 and SD140. Thus, it indicated that miR171b-3p probably regulated the change of anthocyanin biosynthesis in SD92 and SD140 through DELLA protein.

miR828 are frequently reported to be involved in anthocyanin biosynthesis regulation (*Bonar et al., 2018*; *Tirumalai et al., 2019*). In potato, miR828 is associated with purple tuber skin and flesh color rich in anthocyanin. One member of miR828 family, miR828a_1, was identified in SD92 and SD140, but was not significantly expressed differentially between SD92 and SD140. These results indicated that miR828a_1 might not regulate the change of anthocyanin biosynthesis between SD92 and SD140.

The accumulation of anthocyanin is reported to be related with miR156 (*Gou et al., 2011*). In this study, miRNA156 was differentially expressed between SD92 and SD140. Its target gene mainly encoded squamosa promoter binding protein and cell cycle checkpoint protein RAD17. These target genes regulated by miR156a-5p need further study in anthocyanin biosynthesis.

A novel miRNA, novel_mir170, was down-regulated in SD140 (4.81 *vs* 0.14). It regulated a number of target genes, which mainly encoded protein kinase, ethylene responsive transcription factor ERF039-like and transcription factor MYB35-like. Protein kinases play an important role in anthocyanin biosynthesis. Plant sucrose-nonfermenting 1 (SNF1)-related protein kinase is involved in anthocyanin accumulation regulated by MdbHLH3 (*Liu et al., 2017*; *Shen et al., 2017*). Anthocyanin biosynthesis is regulated by mitogen-activated protein kinase (*Luo et al., 2017*; *Wersch, Gao & Zhang, 2018*). In this experiment, the two target genes of novel_mir170 encoding LRR receptor-like serine/threonine-protein kinase were up-regulated, which were consistent with the metabolism data (*Liu et al., 2022*). These results showed that novel_mir170 regulated the change of anthocyanin biosynthesis through LRR receptor-like serine/threonine-protein kinase in SD92 and SD140. MYB transcription factor can regulate the biosynthesis of anthocyanin by regulating the expression of structural genes (*D'Amelia et al., 2014*). The target gene of novel_mir170, which encoded MYB transcription factor, was up-regulated. These results showed that novel_mir170 regulated the anthocyanin biosynthesis by regulating the expression of MYB. Ethylene is closely

related to the biosynthesis of anthocyanin (*Chen et al., 2022*; *Jeong et al., 2010*). In this study, the target gene of novel_mir170 encoding ethylene responsive transcription factor ERF039 was up-regulated. These results indicated that novel_mir170 regulated anthocyanin biosynthesis by up-regulating the expression of ethylene responsive transcription factor. In conclusion, novel_mir170 was an important novel miRNA identified in this study and might be an important miRNA for regulation of anthocyanin biosynthesis.

CONCLUSIONS

A comparative small RNA sequencing analysis between purple potato and its mutant revealed that there were 179 differentially expressed miRNAs, consisting of 65 up- and 114 down-regulated miRNAs, respectively. miR399 and miR172 families were the two largest differentially expressed miRNA families. A total of 31 differentially expressed miRNAs were predicted to potentially regulate 305 target genes. The miRNA sequencing data and the transcriptome data showed that miR171 family and miR172 family regulated the change in anthocyanin biosynthesis from petunidin to pelargonidin through DELLA protein and AP2-like transcription factor, respectively. A novel miRNA, novel_mir170, regulated anthocyanin biosynthesis by serine/threonine-protein kinase and MYB transcription factor.

ACKNOWLEDGEMENTS

We sincerely appreciate Dr. Yumeng Huo for his help in designing miRNA primers for RT-qPCR.

ADDITIONAL INFORMATION AND DECLARATIONS

Funding

This work was supported by the National Natural Science Foundation of China (Grant No. 31901589), the Modern Agriculture Industrial Technology System Funding of Shandong Province (Grant No. SDAIT-16-05), and the "333" Project of Shandong Academy of Agricultural Sciences-Molecular Breeding of Vegetables and Flowers (Grant No. CXGC2021B17). The funders had no role in study design, data collection and analysis, decision to publish, or preparation of the manuscript.

Grant Disclosures

The following grant information was disclosed by the authors:
National Natural Science Foundation of China: 31901589.
Modern Agriculture Industrial Technology System Funding of Shandong Province: SDAIT-16-05.
"333" Project of Shandong Academy of Agricultural Sciences-Molecular Breeding of Vegetables and Flowers: CXGC2021B17.

Competing Interests

The authors declare there are no competing interests.

Author Contributions

- Fang Liu performed the experiments, analyzed the data, prepared figures and/or tables, and approved the final draft.
- Peng Zhao performed the experiments, analyzed the data, authored or reviewed drafts of the article, and approved the final draft.
- Guangxia Chen performed the experiments, prepared figures and/or tables, and approved the final draft.
- Yongqiang Wang performed the experiments, authored or reviewed drafts of the article, and approved the final draft.
- Yuanjun Yang conceived and designed the experiments, authored or reviewed drafts of the article, and approved the final draft.

Data Availability

The following information was supplied regarding data availability:

The data is available at NCBI: PRJNA824931.

Supplemental Information

Supplemental information for this article can be found online at http://dx.doi.org/10.7717/peerj.15349#supplemental-information.

REFERENCES

Abdi H. 2007. The Bonferonni and Šidák corrections for multiple comparisons. In: *Encyclopedia of measurement and statistics*. Thousand Oaks: SAGE.

Axtell MJ. 2013. Classification and comparison of small RNAs from plants. *Annual Review of Plant Biology* **64**:137–159 DOI 10.1146/annurev-arplant-050312-120043.

Balint G, Reynolds AG. 2013. Impact of exogenous abscisic acid on vine physiology and grape composition of Cabernet Sauvignon. *American Journal of Enology and Viticulture* **64**:74–87 DOI 10.5344/ajev.2012.12075.

Bimpilas A, Panagopoulou M, Tsimogiannis D, Oreopoulou V. 2016. Anthocyanin copigmentation and color of wine: the effect of naturally obtained hydroxycinnamic acids as cofactors. *Food Chemistry* **197**:39–46 DOI 10.1016/j.foodchem.2015.10.095.

Bonar N, Liney M, Zhang R, Austin C, Dessoly J, Davidson D, Stephens J, McDougall G, Taylor M, Bryan GJ, Hornyik C. 2018. Potato mir828 is associated with purple tuber skin and flesh color. *Frontiers in Plant Science* **9**:1742 DOI 10.3389/fpls.2018.01742.

Boyle EI, Weng S, Gollub J, Jin H, Botstein D, Cherry JM, Sherlock G. 2004. GO::TermFinder–open source software for accessing Gene Ontology information and finding significantly enriched Gene Ontology terms associated with a list of genes. *Bioinformatics* **20**:3710–3715 DOI 10.1093/bioinformatics/bth456.

Chai Z, Fang J, Huang C, Huang R, Tan X, Chen B, Yao W, Zhang M. 2022. ScAIL1 modulates plant defense responses by targeting DELLA and regulating GA and JA signaling. *Journal of Experimental Botany* **73**:6727–6743 DOI 10.1093/jxb/erac339.

Chen X. 2009. Small RNAs and their roles in plant development. *Annual Review of Cell and Developmental Biology* **25**:21–44 DOI 10.1146/annurev.cellbio.042308.113417.

Chen M, Gu H, Wang L, Shao Y, Li R, Li W. 2022. Exogenous ethylene promotes peel color transformation by regulating the degradation of chlorophyll and synthesis of anthocyanin in postharvest mango fruit. *Frontiers in Nutrition* **9**:911542 DOI 10.3389/fnut.2022.911542.

Chen YF, Shibu MA, Fan MJ, Chen MC, Viswanadha VP, Lin YL, Lai CH, Lin KH, Ho TJ, Kuo WW, Huang CY. 2016. Purple rice anthocyanin extract protects cardiac function in STZ-induced diabetes rat hearts by inhibiting cardiac hypertrophy and fibrosis. *Journal of Nutritional Biochemistry* **31**:98–105 DOI 10.1016/j.jnutbio.2015.12.020.

Chen Y, Wu P, Zhao Q, Tang Y, Chen Y, Li M, Jiang H, Wu G. 2018. Overexpression of a phosphate starvation response AP2/ERF gene from physic nut in Arabidopsis alters root morphological traits and phosphate starvation-induced anthocyanin accumulation. *Frontiers in Plant Science* **9**:1186 DOI 10.3389/fpls.2018.01186.

Chiu LW, Zhou X, Burke S, Wu X, Prior RL, Li L. 2010. The purple cauliflower arises from activation of a MYB transcription factor. *Plant Physiology* **154**:1470–1480 DOI 10.1104/pp.110.164160.

Cristani M, Speciale A, Mancari F, Arcoraci T, Ferrari D, Fratantonio D, Saija A, Cimino F, Trombetta D. 2016. Protective activity of an anthocyanin-rich extract from bilberries and blackcurrants on acute acetaminophen-induced hepatotoxicity in rats. *Natural Product Research* **30**:2845–2849 DOI 10.1080/14786419.2016.1160235.

D'Amelia V, Aversano R, Batelli G, Caruso I, Moreno MCastellano, Castro-Sanz AB, Chiaiese P, Fasano C, Palomba F, Carputo D. 2014. High AN1 variability and interaction with basic helix-loop-helix co-factors related to anthocyanin biosynthesis in potato leaves. *The Plant Journal* **80**:527–540 DOI 10.1111/tpj.12653.

De Jong WS, De Jong DM, De Jong H, Kalazich J, Bodis M. 2003. An allele of dihydroflavonol 4-reductase associated with the ability to produce red anthocyanin pigments in potato (*Solanum tuberosum* L.). *Theoretical and Applied Genetics* **107**:1375–1383 DOI 10.1007/s00122-003-1395-9.

Ding T, Tomes S, Gleave AP, Zhang H, Dare AP, Plunkett B, Espley RV, Luo Z, Zhang R, Allan AC, Zhou Z, Wang H, Wu M, Dong H, Liu C, Liu J, Yan Z, Yao JL. 2022. microRNA172 targets APETALA2 to regulate flavonoid biosynthesis in apple (*Malus domestica*). *Horticulture Research* **9**:uhab007 DOI 10.1093/hr/uhab007.

Evers M, Huttner M, Dueck A, Meister G, Engelmann JC. 2015. miRA: adaptable novel miRNA identification in plants using small RNA sequencing data. *BMC Bioinformatics* **16**:370 DOI 10.1186/s12859-015-0798-3.

Fahlgren N, Carrington JC. 2010. miRNA target prediction in plants. *Methods in Molecular Biology* **592**:51–57 DOI 10.1007/978-1-60327-005-2_4.

Ghorecha V, Patel K, Ingle S, Sunkar R, Krishnayya NS. 2014. Analysis of biochemical variations and microRNA expression in wild (*Ipomoea campanulata*) and cultivated

(*Jacquemontia pentantha*) species exposed to *in vivo* water stress. *Physiology and Molecular Biology of Plants* **20**:57–67 DOI 10.1007/s12298-013-0207-1.

Gou JY, Felippes FF, Liu CJ, Weigel D, Wang JW. 2011. Negative regulation of anthocyanin biosynthesis in Arabidopsis by a miR156-targeted SPL transcription factor. *Plant Cell* **23**:1512–1522 DOI 10.1105/tpc.111.084525.

Han KH, Hashimoto N, Hashimoto M, Noda T, Shimada K, Lee CH, Sekikawa M, Fukushima M. 2006. Red potato extract protects from D-galactosamine-induced liver injury in rats. *Bioscience, Biotechnology, and Biochemistry* **70**:2285–2288 DOI 10.1271/bbb.60097.

He L, Tang R, Shi X, Wang W, Cao Q, Liu X, Wang T, Sun Y, Zhang H, Li R, Jia X. 2019. Uncovering anthocyanin biosynthesis related microRNAs and their target genes by small RNA and degradome sequencing in tuberous roots of sweetpotato. *BMC Plant Biology* **19**:232 DOI 10.1186/s12870-019-1790-2.

Hsieh LC, Lin SI, Shih AC, Chen JW, Lin WY, Tseng CY, Li WH, Chiou TJ. 2009. Uncovering small RNA-mediated responses to phosphate deficiency in Arabidopsis by deep sequencing. *Plant Physiology* **151**:2120–2132 DOI 10.1104/pp.109.147280.

Hu Y, Cheng H, Zhang Y, Zhang J, Niu S, Wang X, Li W, Zhang J, Yao Y. 2021. The MdMYB16/MdMYB1-miR7125-MdCCR module regulates the homeostasis between anthocyanin and lignin biosynthesis during light induction in apple. *New Phytologist* **231**:1105–1122 DOI 10.1111/nph.17431.

Jagla B, Aulner N, Kelly PD, Song D, Volchuk A, Zatorski A, Shum D, Mayer T, De Angelis DA, Ouerfelli O, Rutishauser U, Rothman JE. 2005. Sequence characteristics of functional siRNAs. *RNA* **11**:864–872 DOI 10.1261/rna.7275905.

Jeong SW, Das PK, Jeoung SC, Song JY, Lee HK, Kim YK, Kim WJ, Park YI, Yoo SD, Choi SB, Choi G, Park YI. 2010. Ethylene suppression of sugar-induced anthocyanin pigmentation in Arabidopsis. *Plant Physiology* **154**:1514–1531 DOI 10.1104/pp.110.161869.

Ji XH, Wang YT, Zhang R, Wu SJ, An MM, Li M, Wang CZ, Chen XL, Zhang YM, Chen XS. 2015. Effect of auxin, cytokinin and nitrogen on anthocyanin biosynthesis in callus cultures of red-fleshed apple (*Malus sieversii f. niedzwetzkyana*). *Plant Cell, Tissue and Organ Culture* **120**:325–337 DOI 10.1007/s11240-014-0609-y.

Jia X, Shen J, Liu H, Li F, Ding N, Gao C, Pattanaik S, Patra B, Li R, Yuan L. 2015. Small tandem target mimic-mediated blockage of microRNA858 induces anthocyanin accumulation in tomato. *Planta* **242**:283–293 DOI 10.1007/s00425-015-2305-5.

Jiang C, Gao X, Liao L, Harberd NP, Fu X. 2007. Phosphate starvation root architecture and anthocyanin accumulation responses are modulated by the gibberellin-DELLA signaling pathway in Arabidopsis. *Plant Physiology* **145**:1460–1470 DOI 10.1104/pp.107.103788.

Jones-Rhoades MW, Bartel DP, Bartel B. 2006. MicroRNAs and their regulatory roles in plants. *Annual Review of Plant Biology* **57**:19–53 DOI 10.1146/annurev.arplant.57.032905.105218.

Jung CS, Griffiths HM, De Jong DM, Cheng S, Bodis M, Kim TS, De Jong WS. 2009. The potato developer (D) locus encodes an R2R3 MYB transcription factor that regulates expression of multiple anthocyanin structural genes in tuber skin. *Theoretical and Applied Genetics* **120**:45–57 DOI 10.1007/s00122-009-1158-3.

Jung CS, Griffiths HM, De Jong DM, Cheng S, Bodis M, De Jong WS. 2005. The potato P locus codes for flavonoid 3′, 5′-hydroxylase. *Theoretical and Applied Genetics* **110**:269–275 DOI 10.1007/s00122-004-1829-z.

Kanehisa M, Araki M, Goto S, Hattori M, Hirakawa M, Itoh M, Katayama T, Kawashima S, Okuda S, Tokimatsu T, Yamanishi Y. 2008. KEGG for linking genomes to life and the environment. *Nucleic Acids Research* **36**:D480–D484 DOI 10.1093/nar/gkm882.

Kozomara A, Griffiths-Jones S. 2014. miRBase: annotating high confidence microRNAs using deep sequencing data. *Nucleic Acids Research* **42**:D68–D73 DOI 10.1093/nar/gkt1181.

Langmead B, Trapnell C, Pop M, Salzberg SL. 2009. Ultrafast and memory-efficient alignment of short DNA sequences to the human genome. *Genome Biology* **10**:R25 DOI 10.1186/gb-2009-10-3-r25.

Leão P, Lima M, Costa J, Trindade D. 2014. Abscisic acid and ethephon for improving red color and quality of crimson seedless grapes grown in a tropical region. *American Journal of Enology and Viticulture* **66**:37–45 DOI 10.5344/ajev.2014.14041.

Li Y, Cui W, Wang R, Lin M, Zhong Y, Sun L, Qi X, Fang J. 2019. MicroRNA858-mediated regulation of anthocyanin biosynthesis in kiwifruit (*Actinidia arguta*) based on small RNA sequencing. *PLOS ONE* **14**:e0217480 DOI 10.1371/journal.pone.0217480.

Li S, Wang W, Gao J, Yin K, Wang R, Wang C, Petersen M, Mundy J, Qiu JL. 2016. MYB75 phosphorylation by MPK4 is required for light-induced anthocyanin accumulation in Arabidopsis. *Plant Cell* **28**:2866–2883 DOI 10.1105/tpc.16.00130.

Liu XJ, An XH, Liu X, Hu DG, Wang XF, You CX, Hao YJ. 2017. MdSnRK1.1 interacts with MdJAZ18 to regulate sucrose-induced anthocyanin and proanthocyanidin accumulation in apple. *Journal of Experimental Botany* **68**:2977–2990 DOI 10.1093/jxb/erx150.

Liu F, Chen G, Zhang Y, Zhao P, Dong D, Wang Y, Wang S, Yang Y. 2022. A comparative analysis of metabolome reveals the regulation of the anthocyanin biosynthesis branch in potatoes. *Potato Research* **66**:1–20 DOI 10.1007/s11540-022-09586-5.

Liu Y, Lin-Wang K, Deng C, Warran B, Wang L, Yu B, Yang H, Wang J, Espley RV, Zhang J, Wang D, Allan AC. 2015. Comparative transcriptome analysis of white and purple potato to identify genes involved in anthocyanin biosynthesis. *PLOS ONE* **10**:e0129148 DOI 10.1371/journal.pone.0129148.

Liu Y, Lin-Wang K, Espley RV, Wang L, Li Y, Liu Z, Zhou P, Zeng L, Zhang X, Zhang J, Allan AC. 2019. StMYB44 negatively regulates anthocyanin biosynthesis at high temperatures in tuber flesh of potato. *Journal of Experimental Botany* **70**:3809–3824 DOI 10.1093/jxb/erz194.

Liu Y, Lin-Wang K, Espley RV, Wang L, Yang H, Yu B, Dare A, Varkonyi-Gasic E, Wang J, Zhang J, Wang D, Allan AC. 2016. Functional diversification of the potato R2R3 MYB anthocyanin activators AN1, MYBA1, and MYB113 and their interaction with basic helix-loop-helix cofactors. *Journal of Experimental Botany* **67**:2159–2176 DOI 10.1093/jxb/erw014.

Liu Z, Shi MZ, Xie DY. 2014. Regulation of anthocyanin biosynthesis in Arabidopsis thaliana red pap1-D cells metabolically programmed by auxins. *Planta* **239**:765–781 DOI 10.1007/s00425-013-2011-0.

Liu F, Yang Y, Gao J, Ma C, Bi Y. 2018. A comparative transcriptome analysis of a wild purple potato and its red mutant provides insight into the mechanism of anthocyanin transformation. *PLOS ONE* **13**:e0191406 DOI 10.1371/journal.pone.0191406.

Loreti E, Povero G, Novi G, Solfanelli C, Alpi A, Perata P. 2008. Gibberellins, jasmonate and abscisic acid modulate the sucrose-induced expression of anthocyanin biosynthetic genes in Arabidopsis. *New Phytologist* **179**:1004–1016 DOI 10.1111/j.1469-8137.2008.02511.x.

Luo J, Wang X, Feng L, Li Y, He JX. 2017. The mitogen-activated protein kinase kinase 9 (MKK9) modulates nitrogen acquisition and anthocyanin accumulation under nitrogen-limiting condition in Arabidopsis. *Biochemical and Biophysical Research Communications* **487**:539–544 DOI 10.1016/j.bbrc.2017.04.065.

Matzke M, Kanno T, Daxinger L, Huettel B, Matzke AJ. 2009. RNA-mediated chromatin-based silencing in plants. *Current Opinion in Cell Biology* **21**:367–376 DOI 10.1016/j.ceb.2009.01.025.

Nawrocki EP, Burge SW, Bateman A, Daub J, Eberhardt RY, Eddy SR, Floden EW, Gardner PP, Jones TA, Tate J, Finn RD. 2015. Rfam 12.0: updates to the RNA families database. *Nucleic Acids Research* **43**:D130–D137 DOI 10.1093/nar/gku1063.

Nawrocki EP, Eddy SR. 2013. Infernal 1.1: 100-fold faster RNA homology searches. *Bioinformatics* **29**:2933–2935 DOI 10.1093/bioinformatics/btt509.

Palma-Silva C, Ferro M, Bacci M, Turchetto-Zolet AC. 2016. *De novo* assembly and characterization of leaf and floral transcriptomes of the hybridizing bromeliad species (*Pitcairnia* spp.) adapted to neotropical inselbergs. *Molecular Ecology Resources* **16**:1012–1022 DOI 10.1111/1755-0998.12504.

Saeed AI, Sharov V, White J, Li J, Liang W, Bhagabati N, Braisted J, Klapa M, Currier T, Thiagarajan M, Sturn A, Snuffin M, Rezantsev A, Popov D, Ryltsov A, Kostukovich E, Borisovsky I, Liu Z, Vinsavich A, Trush V, Quackenbush J. 2003. TM4: a free, open-source system for microarray data management and analysis. *Biotechniques* **34**:374–378 DOI 10.2144/03342mt01.

Shen X, Guo X, Zhao D, Zhang Q, Jiang Y, Wang Y, Peng X, Wei Y, Zhai Z, Zhao W, Li T. 2017. Cloning and expression profiling of the PacSnRK2 and PacPP2C gene families during fruit development, ABA treatment, and dehydration stress in sweet cherry. *Plant Physiology and Biochemistry* **119**:275–285 DOI 10.1016/j.plaphy.2017.08.025.

Sukiran NA, Pollastri S, Steel PG, Knight MR. 2022. Plant growth promotion by the interaction of a novel synthetic small molecule with GA-DELLA function. *Plant Direct* **6**:e398 DOI 10.1002/pld3.398.

't Hoen PA, Ariyurek Y, Thygesen HH, Vreugdenhil E, Vossen RH, De Menezes RX, Boer JM, Van Ommen GJ, Den Dunnen JT. 2008. Deep sequencing-based expression analysis shows major advances in robustness, resolution and inter-lab portability over five microarray platforms. *Nucleic Acids Research* **36**:e141 DOI 10.1093/nar/gkn705.

Tirumalai V, Swetha C, Nair A, Pandit A, Shivaprasad PV. 2019. miR828 and miR858 regulate VvMYB114 to promote anthocyanin and flavonol accumulation in grapes. *Journal of Experimental Botany* **70**:4775–4792 DOI 10.1093/jxb/erz264.

Wang L, Feng Z, Wang X, Wang X, Zhang X. 2010. DEGseq: an R package for identifying differentially expressed genes from RNA-seq data. *Bioinformatics* **26**:136–138 DOI 10.1093/bioinformatics/btp612.

Wang Y, Wang Y, Song Z, Zhang H. 2016. Repression of MYBL2 by both microRNA858a and HY5 leads to the activation of anthocyanin biosynthetic pathway in Arabidopsis. *Molecular Plant* **9**:1395–1405 DOI 10.1016/j.molp.2016.07.003.

Wersch RV, Gao F, Zhang Y. 2018. Mitogen-activated protein kinase kinase 6 negatively regulates anthocyanin induction in Arabidopsis. *Plant Signaling & Behavior* **13**:e1526000 DOI 10.1080/15592324.2018.1526000.

Wu HJ, Ma YK, Chen T, Wang M, Wang XJ. 2012. PsRobot: a web-based plant small RNA meta-analysis toolbox. *Nucleic Acids Research* **40**:W22–W28 DOI 10.1093/nar/gks554.

Xia R, Zhu H, An YQ, Beers EP, Liu Z. 2012. Apple miRNAs and tasiRNAs with novel regulatory networks. *Genome Biology* **13**:R47 DOI 10.1186/gb-2012-13-6-r47.

Yang YH, Dudoit S, Luu P, Lin DM, Peng V, Ngai J, Speed TP. 2002. Normalization for cDNA microarray data: a robust composite method addressing single and multiple slide systematic variation. *Nucleic Acids Research* **30**:e15 DOI 10.1093/nar/30.4.e15.

Yoshihama M, Nakao A, Kenmochi N. 2013. snOPY: a small nucleolar RNA orthological gene database. *BMC Research Notes* **6**:426 DOI 10.1186/1756-0500-6-426.

Zhang Y, Liu Z, Liu R, Hao H, Bi Y. 2011. Gibberellins negatively regulate low temperature-induced anthocyanin accumulation in a HY5/HYH-dependent manner. *Plant Signaling & Behavior* **6**:632–634 DOI 10.4161/psb.6.5.14343.